Green Chemistry

PAPER

Cite this: *Green Chem.*, 2025, **27**, 8848

Ambient mechanosynthesis of flexible two-dimensional covalent organic frameworks†

Yogendra Nailwal, [a] Bryson Baker,[b] Ziad Alsudairy, [a,c] Mustapha El Hariri El Nokab, [d] Qingsong Zhang,[e] Tuo Wang, [d] Songliang Cai, [f] Yi Liu [e] and Xinle Li *[a]

Received 8th April 2025,
Accepted 20th June 2025

DOI: 10.1039/d5gc01728a

rsc.li/greenchem

Flexible two-dimensional covalent organic frameworks (2D COFs) constructed from nonplanar building blocks represent an emerging paradigm in COF design. Nevertheless, the prevailing solvothermal synthesis suffers from low time efficiency, environmental unfriendliness, and cumbersome protocols. Here, we address these challenges by developing the first ambient mechanosynthesis of a diverse library of flexible 2D COFs. Sixteen distinct triazine-cored Schiff-base COFs, including five as-yet-unreported ones, were rapidly synthesized *via* ball milling using 2,4,6-tris(4-aminophenoxy)-1,3,5-triazine (TPT-NH_2) and 2,4,6-tris(4-formylphenoxy)-1,3,5-triazine (TPT-CHO) as building blocks. Notably, the representative COF, MC-flexible-COF-1, was synthesized in as little as one hour under mechanosynthesis conditions, whereas it remained unattainable *via* the traditional solvothermal method, despite prolonged heating and extensive solvent screening. The highly dynamic nature of the imine linkage was unequivocally demonstrated through mechanochemical "scrambling" experiments using molecular model compounds. Furthermore, MC-flexible-COF-1 exhibited a high iodine uptake capacity of ~4.30 g g^{-1} from aqueous solutions and 5.97 g g^{-1} from the vapor phase. This work underscores the immense potential of mechanochemistry as a powerful and sustainable tool for the rapid synthesis of advanced 2D COFs, including those inaccessible *via* conventional solution-based methods.

Green foundation

1. We report the first ambient, rapid, liquid-assisted mechanosynthesis of flexible Schiff-base 2D covalent organic frameworks (COFs). A diverse library of 16 COFs was synthesized in just one hour at room temperature with minimal solvent usage.
2. One representative flexible COF displayed exceptional iodine adsorption capabilities of 4.3 ± 0.2 g g^{-1} toward aqueous triiodide and 5.97 g g^{-1} for iodine vapor, which underscores the significant potential of flexible COF adsorbents for radioactive iodine capture.
3. Looking forward, mechanochemistry promises to offer an environmentally benign and efficient synthetic route to novel COFs, including those that have historically been difficult to access *via* conventional solution-based methods.

Introduction

Two-dimensional covalent organic frameworks (2D COFs) are layered crystalline, porous, polymer networks interlinked by strong covalent bonds.[1] Their inherent structural attributes such as light weight, high porosity, well-ordered skeletons, customizable functionalities, and outstanding stability, make them highly appealing for a wide array of applications, including gas separation,[2] heterogeneous catalysis,[3] drug delivery,[4] energy storage,[5] sensing,[6] environmental remediation,[7] proton conduction,[8] among others. 2D COFs are typically constructed from rigid, planar organic building blocks, which restrict rotational freedom and thus minimize the occurrence of structural defects, such as extended faults and packing errors during crystallization.[9] While the use of rigid monomers is

[a]*Department of Chemistry, Clark Atlanta University, Atlanta, Georgia 30314, USA. E-mail: xli1@cau.edu*
[b]*Department of Chemistry, Howard University, Washington, DC 20059, USA*
[c]*Department of Chemistry, College of Science, Qassim University, Buraidah 51452, Saudi Arabia*
[d]*Department of Chemistry, Michigan State University, East Lansing, Michigan 48824, USA*
[e]*The Molecular Foundry, Lawrence Berkeley National Laboratory, One Cyclotron Road, Berkeley, California 94720, USA*
[f]*Guangzhou Key Laboratory of Analytical Chemistry for Biomedicine, School of Chemistry, South China Normal University, Guangzhou 510006, P. R. China*
† Electronic supplementary information (ESI) available. See DOI: https://doi.org/10.1039/d5gc01728a

essential for achieving the high crystallinity of 2D COFs, it also limits their structural diversity and flexibility. To this end, developing novel COFs from flexible building blocks has garnered substantial attention in recent years. Extensive research efforts have been devoted to synthesizing COFs using flexible building units, particularly those based on 2,4,6-triaryloxy-1,3,5-triazine, such as 2,4,6-tris(4-formylphenoxy)-1,3,5-triazine (TPT-CHO) and 2,4,6-tris(4-aminophenoxy)-1,3,5-triazine (TPT-NH_2). The emergent class of flexible 2D COFs with a triazine-core exhibit unique physicochemical properties that have demonstrated significant potential for diverse applications.[10] For instance, Zhang and co-workers reported a luminescent flexible 2D COF derived from TPT-CHO, showing highly sensitive and selective detection of picric acid.[11] Most recently in 2024, Pandey and co-workers developed four flexible 2D COFs with a triazine-core that exhibited exceptional performance in supercapacitor and CO_2 capture.[12] Despite these substantial strides, the synthesis of flexible 2D COFs predominantly relies on solvothermal methods, which suffer from key drawbacks including long reaction times (typically 3 days), high energy consumption, adverse environmental effects due to the use of toxic solvents, meticulous reaction setup associated with the deoxygenation process, and limited scalability (Scheme 1).[13] These synthetic barriers have significantly impeded the broad application and structural diversification of flexible COFs. Consequently, there is an urgent need to develop a generic synthetic route to construct flexible COFs under milder conditions.

The past decade has witnessed a surge of scientific interest in exploring ambient and expeditious synthesis methods for COFs.[14] Among these promising strategies, mechanochemistry, a transformative synthetic methodology that harnesses mechanical force to drive chemical transformations, offers notable advantages,[15] including (i) environmental benignity due to minimal solvent usage; (ii) rapid reaction times, ranging from minutes to hours; (iii) operational simplicity by circumventing tedious protocols such as freeze-pump-thaw and flame sealing; (iv) enhanced scalability owing to its solid-state nature; and (v) access to products that are otherwise challenging to obtain through conventional solution-based methods. While the mechanosynthesis of organic molecules, polymers, inorganic nanomaterials, and metal–organic frameworks (MOFs) has been extensively studied for decades,[16–18] the exploration of mechanochemistry in COFs is still in its nascent stage. The first mechanosynthesis of COFs dates back to 2013 when the Banerjee group synthesized three β-ketoenamine-linked 2D COFs using a mortar and pestle.[19] Thereafter, the same group developed the liquid-assisted grinding method (2014) and salt-mediated crystallization approach (2017) in COF mechanochemistry.[20,21] In recent years, COF mechanochemistry has garnered increasing scientific interest, leading to the rapid and sustainable synthesis of various 2D COFs with Schiff-base,[20] triazine,[22] and boroxine[23] linkages, as well as COF composites with metal ions,[24] nanoparticles,[25] enzymes,[26] polyoxometalates,[27] and silica.[28] Despite remarkable progress in greener and faster synthesis of COFs, the full potential of mechanochemistry is impeded by two key factors: the predominant reliance on rigid, planar monomers for 2D COF synthesis and the limited attempts to create COFs inaccessible *via* solution-based methods. To address this gap, we propose that mechanochemistry offers a simple, rapid, and environmentally benign route for synthesiz-

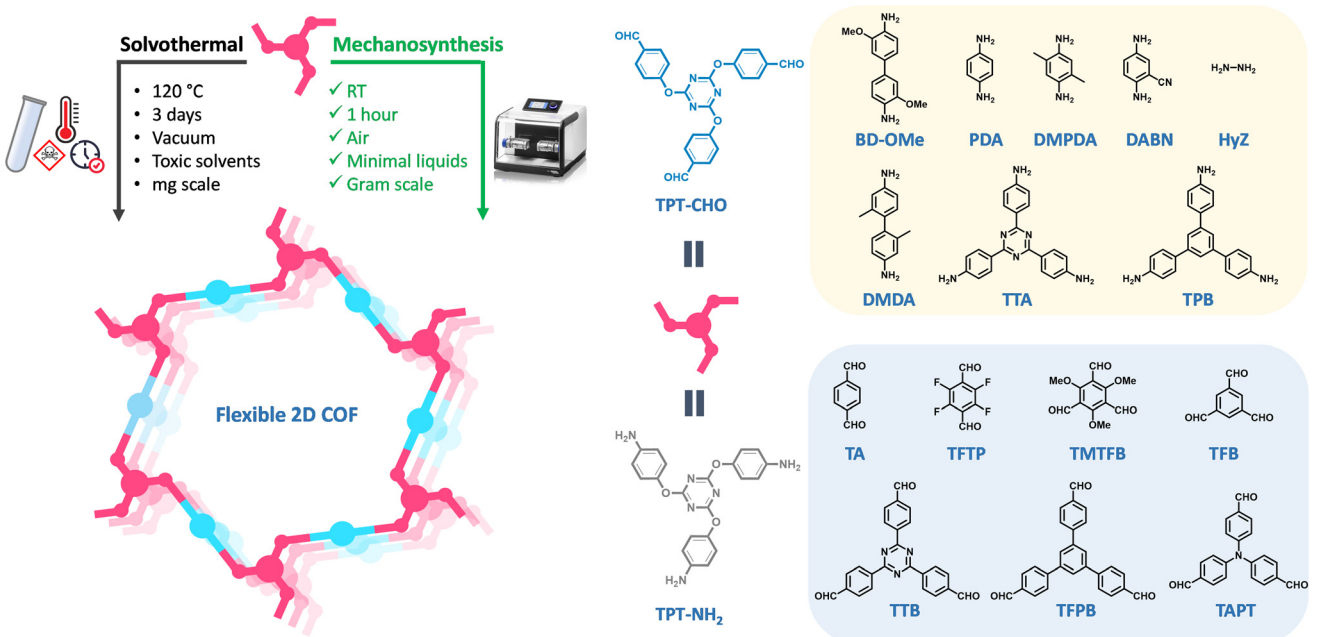

Scheme 1 Schematic representation of ambient, rapid, liquid-assisted mechanosynthesis of flexible triazine-based 2D COFs, in contrast to traditional solvothermal routes.

ing flexible 2D COFs, including those hard to obtain in solution. To the best of our knowledge, the ambient mechanosynthesis of flexible 2D COFs remains hitherto uncharted.

On the other hand, nuclear energy is deemed as one of the most prominent sources of clean energy in the modern world, offering a viable solution to the global energy crisis due to its minimal greenhouse gas emissions. It is widely used in various sectors, including aerospace, energy production, and military applications. However, a major challenge associated with nuclear fission is the generation of radioactive waste, which contains hazardous isotopes that pose significant risks to human health. Among these, radioactive iodine isotopes, particularly ^{129}I and ^{131}I, are among the most common and harmful elements.[29] In the environment, radioactive iodine can exist as iodine vapor in the air and as molecular or ionic species in water ($I_2 + I^- \rightleftharpoons I_3^-$). To mitigate these risks, adsorption-based capture has emerged as a potent strategy and various adsorbents such as activated carbon, silver-exchanged zeolites, MOFs, and porous organic polymers have been explored.[30] In recent years, COFs, particularly flexible COFs, have gained considerable attention for capturing both molecular and ionic iodine species due to their ordered, heteroatom-rich pore structures. For example, Li and co-workers synthesized a series of flexible 2D imine-linked COFs with varying degrees of interlayer hydrogen bonding, achieving excellent iodine vapor uptake of up to 5.43 g g^{-1}.[31] Ma and co-workers developed four flexible amine-linked COFs *via* the Eschweiler–Clarke reaction and achieved a high iodine vapor uptake of 5.49 g g^{-1}.[32] Hashmi and co-workers developed a flexible imine-linked COF adsorbent (NR_COF-C1), which demonstrated outstanding iodine capture capacities in both vapor (5.45 g g^{-1}) and aqueous solutions (4.85 g g^{-1}).[33] Despite these advancements, traditional solvothermal methods for COF adsorbents typically contradict the principles of green chemistry, thereby creating a significant stumbling block to their broader application. Hence, it is of paramount significance to develop environmentally benign synthesis methods for COF-based adsorbents. However, relevant studies remain largely elusive thus far.[34]

In this study, we showcase the first ambient, rapid, liquid-assisted mechanosynthesis of flexible Schiff-base 2D COFs using triazine-based trialdehyde and triamine as primary building blocks (Scheme 1). In total, 16 different COFs bearing varied pore sizes, pendant functionalities, Schiff-base linkages, and core structures, including 5 previously unreported flexible COFs, were prepared in only one hour at room temperature with minimal solvent usage. This method can be easily scaled to the half-gram scale without compromising COF quality. One representative COF was systematically investigated to elucidate the influence of mechanosynthesis parameters. Most notably, this approach enabled the efficient synthesis of a COF inaccessible by traditional solution-phase methods. To shed light on the mechanochemical COF formation, imine exchange reactions of model compounds were utilized to probe the dynamic nature of imine bonds under mechanical force. When used for the adsorption of triiodide from aqueous I_2/KI solution and molecular iodine vapor, MC-flexible-COF-1 displayed a high adsorption capability of 4.3 ± 0.2 g g^{-1} toward aqueous triiodide and 5.97 g g^{-1} for iodine vapor.

Results and discussion

Initially, a flexible imine-linked 2D COF (denoted as MC-flexible-COF-1, where MC represents mechanochemistry), derived from 2,4,6-tris(4-formylphenoxy)-1,3,5-triazine (TPT-CHO) and 3,3′-dimethoxy-[1,1′-biphenyl]-4,4′-diamine (BD-OMe),[35] was selected as a benchmark system to optimize the mechanosynthesis parameters (Fig. 1a). Ambient mechanosynthesis of MC-flexible-COF-1 was conducted by ball-milling TPT-CHO and BD-OMe in a 5 mL stainless steel jar containing one 5 mm stainless steel ball under aerobic conditions (Scheme S1†). To optimize the crystallinity of COF, several synthetic parameters were fine-tuned, including liquid additives, catalyst concentration, milling frequency, and reaction time (Fig. 1). The COF quality was assessed using powder X-ray diffraction (PXRD) analysis. We commenced by optimizing liquid additives for mechanosynthesis, as liquid additives have been demonstrated to enhance the crystallinity of 2D COFs during mechanosynthesis.[36] Neat milling of COF monomers in the absence of any liquid additives only yielded an amorphous product (Fig. S1†), underscoring the vital role liquid additives play in achieving high-quality COFs through mechanosynthesis. A mixture of mesitylene and acetonitrile (ACN) was found to be optimal when compared to mesitylene, ACN, and mesitylene/dioxane (Fig. 1b and Table S1†). Next, the influence of acetic acid (AcOH) catalyst concentration on COF formation was examined. Increasing the AcOH concentration from 6 M to 17.4 M in the presence of mesitylene/ACN progressively enhanced the crystallinity of the resultant COF (Fig. 1c). Similarly, milling frequency plays an essential role in the mechanosynthesis of flexible 2D COFs. Systematic variation of the milling frequency from 5 Hz to 30 Hz revealed an optimum at 20 Hz (Fig. 1d). A too-high milling frequency hampered the COF crystallinity, consistent with our previous work on imine COF mechanosynthesis.[34] To gain a better understanding of the COF formation, a rigorous *ex situ* kinetic study was conducted. Gratifyingly, MC-flexible-COF-1 exhibited a prominent (100) Bragg diffraction peak at 2θ = 2.2° after a mere 1 minute of ball-milling under ambient conditions. The intensity of the characteristic reflections increased progressively at 5, 10, and 30 minutes, reaching their maximum at 1 hour (Fig. 1e). Ultimately, the optimal conditions for ambient mechanosynthesis of MC-flexible-COF-1 were established: mesitylene/ACN as liquid additives (ratio of the liquid additive to the mass of reactants, η = 0.88 μL mg^{-1}), glacial AcOH as the catalyst, a milling frequency of 20 Hz, and a milling time of 1 hour. Under these conditions, powdered MC-flexible-COF-1 was obtained with a dark-yellow color in a high yield of 76% (inset image, Fig. 1a).

To further highlight the advantages of mechanosynthesis, we opted for the preparation of the solvothermal analogue of MC-flexible-COF-1 using traditional solution methods. Despite

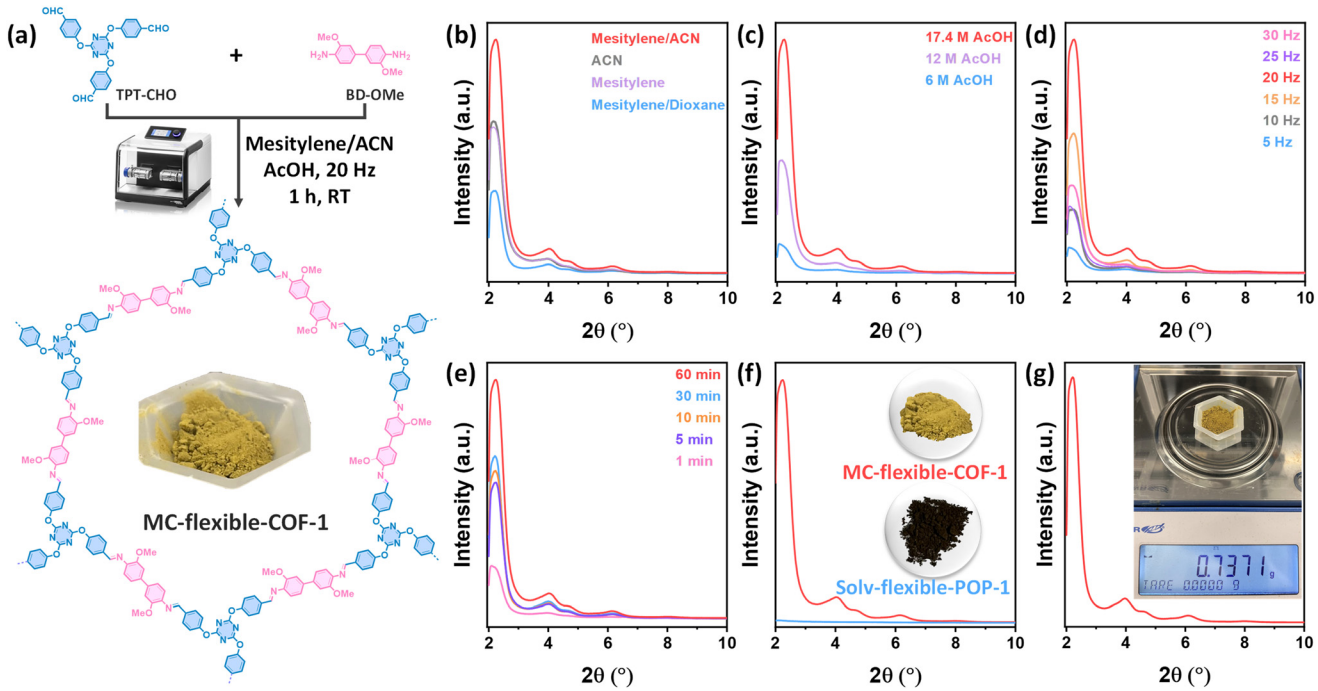

Fig. 1 Ambient mechanosynthesis of MC-flexible-COF-1. (a) Schematic of MC-flexible-COF-1 *via* ball-milling synthesis under ambient conditions. PXRD patterns of MC-flexible-COF-1 with variation of (b) liquid additives, (c) catalyst concentration, (d) milling frequency, and (e) milling time. (f) PXRD patterns of MC-flexible-COF-1 and solv-flexible-POP-1; the inset shows their physical appearance; (g) Gram-scale synthesis of MC-flexible-COF-1.

extensive optimization of solvothermal conditions using aqueous acetic acid as the catalyst (Table S2†), including variations in solvents, acetic acid concentration, reaction times (up to 4 days), atmosphere, and temperatures (80–120 °C), we failed to obtain the crystalline product (Fig. S2†). Under certain conditions, precipitates were not even formed (Table S2†). In stark contrast, the mechanosynthesis enabled the effective synthesis of highly crystalline MC-flexible-COF-1 in as little time as minutes. The PXRD pattern of MC-flexible-COF-1 displayed sharp and distinct diffraction peaks, conspicuously absent in the amorphous solv-flexible-POP-1 (Fig. 1f). Furthermore, their visual differences were striking: MC-flexible-COF-1 exhibited a dark-yellow color whereas solv-flexible-POP-1 appeared deep brown (inset image, Fig. 1f), signifying partial oxidation at elevated temperatures during the solvothermal process. These marked contrasts in physical appearance, crystallinity, and synthetic outcomes underscore the unparalleled advantages of mechanosynthesis, as it not only provides an environmentally benign route to COFs but also enables the synthesis of COFs inaccessible *via* traditional solution-based methods.[15] It is worth noting that MC-flexible-COF-1 powder (a.k.a., EB-COF-6) was obtained in solution under high-energy (1.5 MeV) electron beam irradiation conditions.[35] Moreover, the MC-flexible-COF-1 aerogel (a.k.a., COFA-8) was synthesized using $Sc(OTf)_3$ as the catalyst, followed by freeze-drying, whereas the acetic acid-catalyzed reactions failed to produce gels.[37] These findings align with our observation that it was challenging using acetic acid as the catalyst and the traditional solvothermal method to synthesize MC-flexible-COF-1 powder. To quantitatively evaluate the sustainability benefits of mechanosynthesis, we calculated key green chemistry metrics such as *E*-factor and material intensity (MI). As shown in Table S3,† mechanosynthesis exhibited an *E*-factor of 544.6 and an MI of 545.8, which are markedly lower than those with solvothermal synthesis (*E*-factor = 736.7, MI = 735.2). These results highlight the reduced waste generation and improved sustainability of the mechanosynthesis strategy. In addition, the large-scale synthesis of COFs, a critical prerequisite for industrial applications, has long been a formidable challenge.[38] Given its exceptional scalability in chemical synthesis, mechanochemistry offers a promising solution. To assess the scalability of our mechanosynthesis, a gram-scale reaction was conducted using a 25 mL stainless steel jar, yielding 0.73 g of highly crystalline MC-flexible-COF-1 in just 1 h (Fig. 1g). The synthesis was repeated in different batches with slight variations in ball sizes. The yields and PXRD patterns of the product showed the robustness of the method (Fig. S3 and Table S4†). These results collectively underscore the practicality of mechanosynthesis for the large-scale production of high-quality flexible 2D COFs.

The obtained MC-flexible-COF-1 was thoroughly characterized using a suite of analytical techniques. Fourier transform infrared (FTIR) spectroscopy of MC-flexible-COF-1 showed the significant attenuation of the characteristic –CHO stretching at 1693 cm^{-1} from TPT-CHO and $-NH_2$ stretching at 3429 cm^{-1} from BD-OMe, alongside the emergence of a new

signal for –C═N stretching at 1626 cm^{-1}, indicating successful imine condensation (Fig. 2a). The presence of the imine linkage was further corroborated by solid-state ^{13}C cross-polarization magic angle spinning (CP-MAS) NMR spectroscopy (Fig. 2b). The ^{13}C CP-MAS NMR spectrum of MC-flexible-COF-1 revealed a peak at 157 ppm, corresponding to imine carbon. In addition, the prominent peaks at 174 ppm and 55 ppm were attributed to the triazine carbon and methoxy carbon, respectively.

The crystalline structure of MC-flexible-COF-1 was confirmed by PXRD analysis and structural simulation. The PXRD pattern of MC-flexible-COF-1 revealed five prominent reflection peaks, with the most intense one at 2θ = 2.22° (FWHM = 0.46°) and additional reflections at 2θ = 3.97, 4.57, 6.12, 8.02 and 26.82°, corresponding to the (100), (110), (200), (210), (220), and (001) facets, respectively (Fig. 2c, red curve). We speculate that the formation of the highly crystalline 2D COF from the flexible TPT-CHO monomer is primarily driven by the synergistic effects of dynamic covalent chemistry,[39] constrained monomer flexibility during polymerization,[40] and strong non-covalent interactions imparted by the triaryloxytriazine core.[41] To elucidate the unit cell parameters of MC-flexible-COF-1, eclipse AA and staggered AB stacking modes were modeled in the space group *P*6 (Fig. 2c, inset). The experimental PXRD pattern closely matched the pattern simulated from the AA

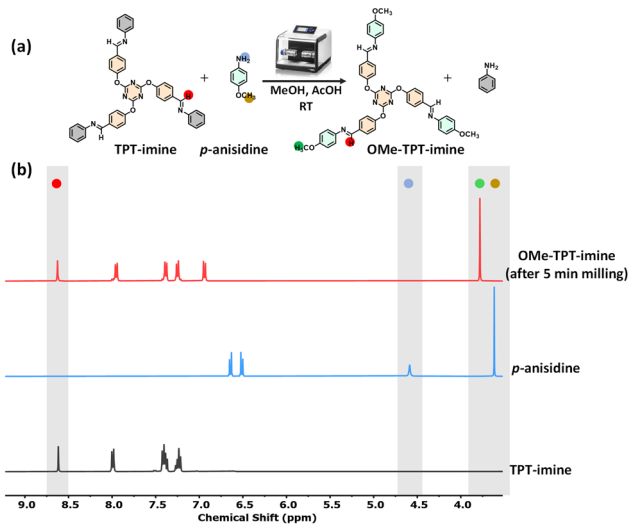

Fig. 3 (a) "Scrambling" experiment between a model imine analog with a triazine-core (TPT-imine) and *p*-anisidine under ball milling conditions. (b) ^{1}H NMR (d^6-DMSO) spectra of the product from mechanosynthesis-enabled imine exchange (red curve), *p*-anisidine (blue curve), and the non-functionalized imine analog, TPT-imine (black curve).

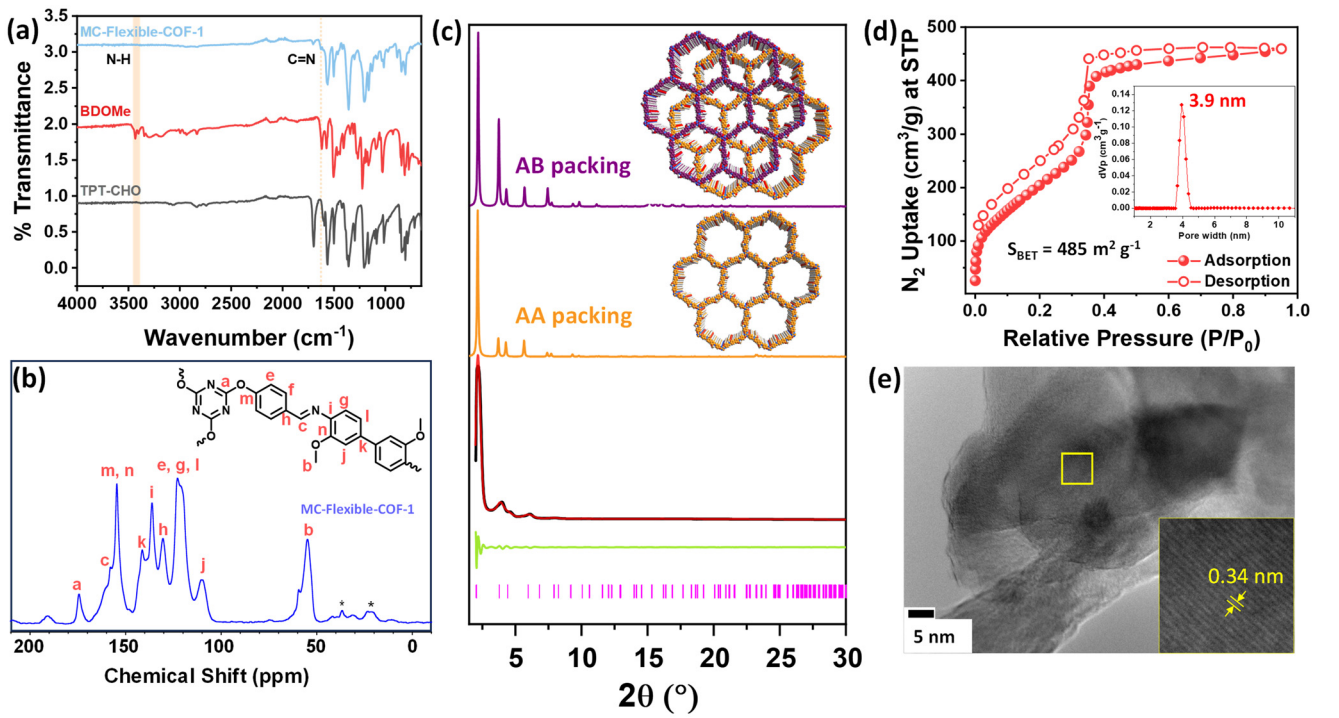

Fig. 2 (a) FTIR spectra of MC-flexible-COF-1, BD-OMe, and TPT-CHO. (b) Solid-state ^{13}C CP-MAS NMR spectrum of MC-flexible-COF-1. Asterisks denote the spinning sidebands. (c) PXRD profiles of MC-flexible-COF-1. Experimental (black), Pawley refined (red), and their difference (green), simulated pattern using the AA stacking mode (orange) and the staggered AB stacking mode (purple). Inset: eclipsed AA and staggered AB stacking structure of MC-flexible-COF-1. (d) N_2 adsorption–desorption isotherms of MC-flexible-COF-1. Inset is the pore size distribution profile calculated by the QSDFT model. (e) TEM images of MC-flexible-COF-1; the inset is a zoomed-in TEM image of the marked yellow area showing periodic lattice fringes.

stacking mode (Fig. 2c, orange curve), whereas it deviated from that for the AB stacking mode (Fig. 2c, purple curve). Furthermore, Pawley refinement provided a good fit to the experimental PXRD pattern (Fig. 2c, red curve), as evidenced by the minimal difference between the simulated and experimental profiles (Fig. 2c, green curve). The Pawley refinement yielded a unit cell of $a = b = 44.63$ Å, $c = 3.48$ Å, $\alpha = \beta = 90°$, $\gamma = 120°$ with good agreement factors ($R_{WP} = 4.68\%$, $R_P = 6.08\%$). The permanent porosity of MC-flexible-COF-1 was evaluated by N_2 uptake analysis. A Type IV sorption isotherm with a hysteresis loop suggested the mesoporous nature of the COF (Fig. 2d). The Brunauer–Emmett–Teller (BET) surface area was calculated as being 485 $m^2\ g^{-1}$ for MC-flexible-COF-1, higher than those obtained in 1-minute and 10-minute milling (Fig. S4 and S5†). The pore size distribution estimated by fitting the N_2 isotherm with the quenched solid density functional theory (QSDFT) model exhibited a pore width centered at 3.9 nm (inset of Fig. 2d), which aligns closely with the predicted pore width for the AA stacking mode. The morphology of MC-flexible-COF-1 was investigated using scanning electron microscopy (SEM) and transmission electron microscopy (TEM). The SEM images revealed the layered aggregates with relative sizes of 30–50 μm for MC-flexible-COF-1 (Fig. S6†). TEM imaging also confirmed the 2D layered sheet morphology and exhibited periodic lattice fringes with a *d*-spacing of 0.34 nm (Fig. 2e and S7†), corresponding to the (001) lattice plane of MC-flexible-COF-1. This value also aligns with the calculated interlayer distance of 0.33 nm from the (001) reflection in the PXRD pattern. Moreover, thermogravimetric analysis (TGA) indicated the high thermal stability of MC-flexible-COF-1 up to 350 °C under anaerobic (N_2) conditions (Fig. S8†).

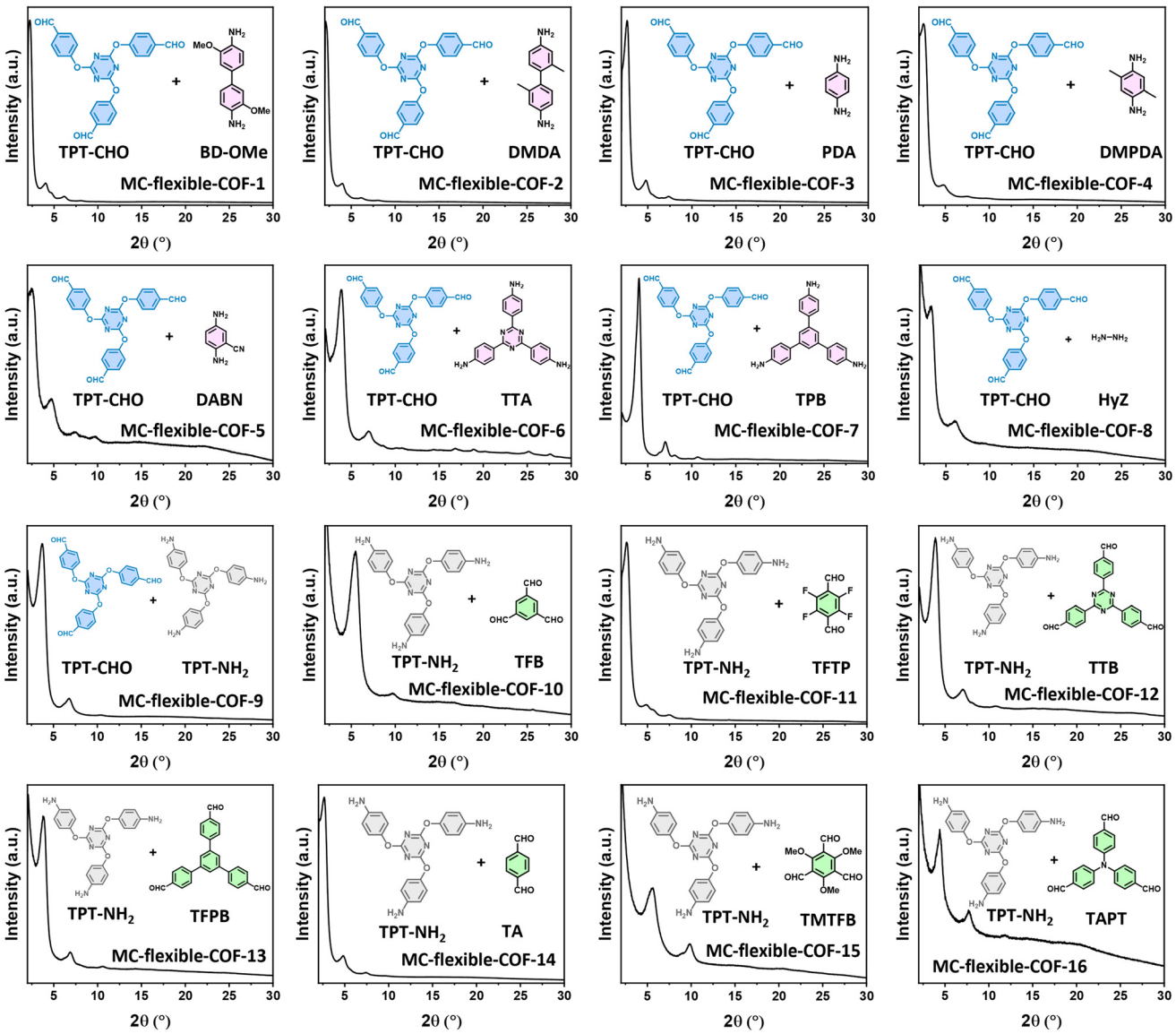

Fig. 4 The broad applicability of mechanosynthesis of 2D MC-flexible-COFs under ambient conditions.

The reversible nature of covalent bonds governs the crystallinity of 2D COFs, as it enables the dynamic breaking and reformation of in-plane bonds within the COF lattice, ultimately driving the system toward its thermodynamic minimum.[39] We hypothesize that the reversibility of imine bonds under mechanosynthesis conditions plays a pivotal role in the rapid formation of flexible COFs. To probe the dynamic nature of imine bonds under ball milling conditions, we performed a "scrambling" experiment between a model imine analog with a triazine-core (TPT-imine) and *p*-anisidine (Fig. 3a). The solid mixture was subjected to ball milling in the presence of catalytic acetic acid under ambient conditions and the resulting products were analyzed by solution-phase ^{1}H NMR spectroscopy. Remarkably, after only 5 minutes of ball-milling, ^{1}H NMR analysis revealed the emergence of a singlet at 3.8 ppm, characteristic of the methoxy group in the newly formed OMe-TPT-imine (Fig. 3b, red curve), confirming the rapid occurrence of the imine exchange reaction under nearly solid-state conditions. This result provides compelling evidence for the highly dynamic nature of imine bonds under mechanochemical conditions, which is poised to be responsible for the rapid formation of highly crystalline flexible 2D COFs.

To showcase the generality of the mechanosynthesis strategy, we synthesized 15 additional flexible 2D COFs from various amine and aldehyde monomers (Fig. 4). These [C_3 + C_2] and [C_3 + C_3] polymerizations were conducted for the construction of 2D COFs with different pore sizes, pendant groups, and Schiff-base linkages (*i.e.*, imine, azine, and β-ketoenamine). Of these, 10 COFs have been previously reported and were predominantly prepared *via* conventional solution-based methods. It is worth noting that the mechanosynthesis strategy enabled the synthesis of these 2D COFs with moderate-to-high crystallinity: TPT-CHO-DMDA (MC-flexible-COF-2),[32] TPT-CHO-PDA (MC-flexible-COF-3),[10] TPT-CHO-TTA (MC-flexible-COF-6),[42] TPT-CHO-TPB (MC-flexible-COF-7),[12] TPT-CHO-HyZ (MC-flexible-COF-8),[43] TPT-CHO-TPT-NH_2 (MC-flexible-COF-9),[12] TPT-NH_2-TFB (MC-flexible-COF-10),[35] TPT-NH_2-TTB (MC-flexible-COF-12),[35] TPT-NH_2-TFPB (MC-flexible-COF-13),[35] and TPT-NH_2-TA (MC-flexible-COF-14).[42] The PXRD profiles (Fig. S9–S23†) and FTIR spectra (Fig. S24†) of the obtained COFs were in good agreement with previous data in the literature. The simulated PXRD patterns of the newly synthesized flexible COFs are closely matched with their experimental PXRD patterns (Fig. S25†). It is noteworthy that MC-flexible-COF-6 and MC-flexible-COF-12, as well as MC-flexible-COF-7 and MC-flexible-COF-13, are isomeric COFs that possess identical compositions but distinct linkage orientations. These COF isomers have recently garnered increasing attention and merit further investigation.[44] Taken together, this mechanosynthesis method is broadly applicable, affording a wide range of flexible 2D COFs under ambient conditions within an hour.

Encouraged by the heteroatom-rich and ordered pore channels of MC-flexible-COFs, we investigated their potential as

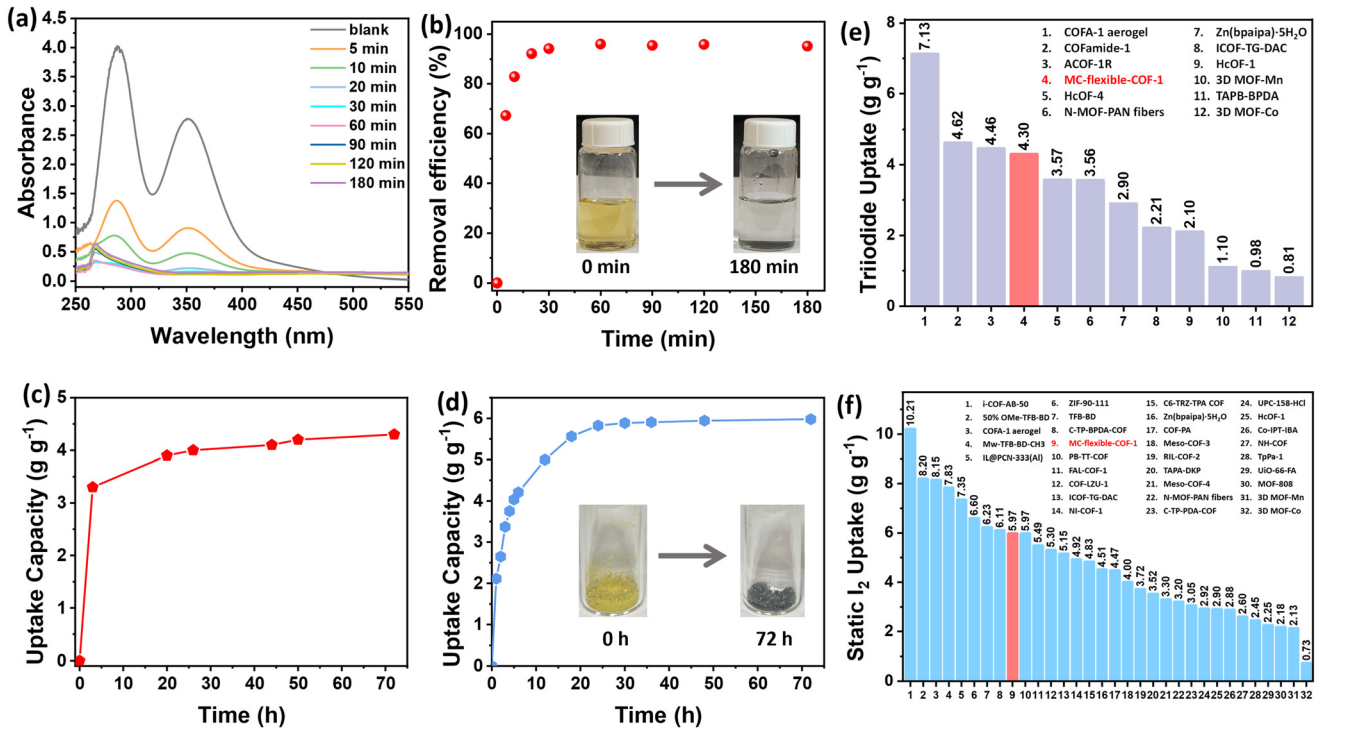

Fig. 5 (a) UV-vis spectra of I_3^- adsorption by MC-flexible-COF-1 in I_2/KI aqueous solution. (b) Removal efficiency of I_3^- by MC-flexible-COF-1. (c) Maximum I_3^- adsorption isotherm of MC-flexible-COF-1 in I_2/KI solution. (d) Time-dependent iodine vapor uptake by MC-flexible-COF-1. Inset: physical appearance of MC-flexible-COF-1 before and after exposure to iodine vapor. Comparison of iodine uptake by MC-flexible-COF-1 with other porous materials (*e.g.*, COFs and MOFs) (e) in an aqueous solution (triiodide (I_3^-) adsorption) and (f) in the vapor phase.

adsorbents for capturing triiodide (I_3^-) from aqueous solutions and iodine vapor. To evaluate this, MC-flexible-COF-1 was introduced into a 10 mL aqueous solution of I_2/KI (150 ppm I_2 and 250 ppm KI), where I_3^- forms *via* the equilibrium reaction $I_2 + I^- \rightleftharpoons I_3^-$. The adsorption process was monitored using UV-vis spectroscopy, tracking the characteristic absorption peaks of I_2 (290 nm) and I_3^- (350 nm) (Fig. 5a). A kinetic study revealed that MC-flexible-COF-1 rapidly removed approximately 80% of iodine within 20 minutes (Fig. 5b). The maximum I_3^- uptake capacity was evaluated by immersing MC-flexible-COF-1 in a concentrated I_2/KI (4 mM) aqueous solution for 3 days. The maximum iodine uptake capacity of MC-flexible-COF-1 was calculated to be 4.3 ± 0.2 g g^{-1} (Fig. 5c), surpassing many previously reported porous adsorbents (Fig. 5e, see a full reference list in Table S20†).[45–51] Adsorption kinetics of MC-flexible-COF-1 were best described by the pseudo-second-order model, exhibiting a high correlation coefficient (R^2) value of 0.999 (Fig. S26†). Furthermore, the selectivity of I_3^- in the iodine solution by MC-flexible-COF-1 was examined in the presence of competing anions such as SO_4^{2-} (K_2SO_4), Cl^- (KCl), NO_3^- (KNO_3), CH_3COO^- (Ac^-, CH_3COOK) and CO_3^{2-} (K_2CO_3). Remarkably, MC-flexible-COF-1 demonstrated excellent selectivity towards I_3^- over these anions, revealing excellent binding affinity for I_3^- (Fig. S27†). The reusability of MC-flexible-COF-1 adsorbent was evaluated by cycling experiments. After each adsorption cycle, MC-flexible-COF-1 was washed with methanol and dried at 120 °C under vacuum for use in the next cycle. It was found that the crystallinity of the COF was retained through the first three cycles. After four cycles, the I_3^- adsorption capability of MC-flexible-COF-1 decreased to 90% of the initial value (Fig. S28†), accompanied by a complete loss of crystallinity in a I_3^--loaded MC-flexible-COF-1 (Fig. S29†). In addition to aqueous iodine capture, the iodine vapor adsorption performance of MC-flexible-COF-1 was also evaluated at 75 °C in a closed vial under ambient pressure. A visible color change from yellow to black upon exposure to iodine vapor indicated successful adsorption by the COF material (inset, Fig. 5d). MC-flexible-COF-1 exhibited a rapid initial uptake of iodine vapor, reaching a high iodine adsorption capacity of 5.97 g g^{-1} within 24 hours (Fig. 5d). This sorption value surpassed the iodine adsorption capacities of many reported porous materials, including COFs,[32,48,52–56] and MOFs.[57–60] (Fig. 5f and see a full reference list in Table S20†).

Conclusions

In conclusion, we have developed the first mechanosynthesis of a diverse library of flexible 2D COFs from triazine-based monomers under ambient conditions. This rapid and nearly solventless method enabled the synthesis of 16 distinct Schiff-base COFs within 1 hour, offering significant advantages over traditional solvothermal methods in terms of efficiency, sustainability, simplicity, scalability, and versatility. Importantly, mechanochemistry enabled the efficient synthesis of MC-flexible-COF-1, which was unattainable through traditional solution-based methods. Mechanochemical imine exchange studies in molecular model compounds have revealed the highly dynamic nature of imine linkage under mechanical force, which plays an essential role in the rapid formation of flexible COFs. Furthermore, MC-flexible-COF-1 demonstrated a high adsorption capability of 4.3 ± 0.2 g g^{-1} for aqueous and 5.97 g g^{-1} vapor iodine pollutants, outperforming numerous previously reported COF adsorbents. This study unlocks the full potential of mechanochemistry for the sustainable and rapid synthesis of novel COFs, thereby expediting their discovery and enhancing their industrial prospects.

Author contributions

Yogendra Nailwal: writing – original draft; visualization; investigation; data curation; and formal analysis. Bryson Baker: investigation and data curation. Ziad Alsudairy: investigation and data curation. Mustapha El Hariri El Nokab: writing – review and editing; data curation; and validation. Qingsong Zhang: data curation and validation. Tuo Wang: writing – review and editing; data curation; resources and supervision. Songliang Cai: writing – review and editing; software; investigation; and data curation. Yi Liu: writing – review and editing; data curation; resources; and supervision. Xinle Li: conceptualization; writing – review and editing; supervision; project administration; methodology; and funding acquisition.

Conflicts of interest

There are no conflicts to declare.

Data availability

The data supporting this article have been included as part of the ESI.†

Acknowledgements

This work is funded by the U.S. Department of Energy Early Career Award (DE-SC0022000), the National Science Foundation HBCU-UP-RIA program (no. 2100360), the PREC program (no. 2216807), and the PREM program (DMR-2122147). B. B. was supported by the Research Experiences for Undergraduates (REU) program under NSF Award No. 2150206. S. C. is grateful for the support from the National Natural Science Foundation of China (no. 22171092). Part of the work was carried out at the Molecular Foundry as a user project, supported by the Office of Science, Office of Basic Energy Sciences, of the U.S. Department of Energy under Contract No. DE-AC02-05CH11231. Solid-state NMR analysis was supported by the National Science Foundation under the grant number MCB-2308660.

References

1 C. S. Diercks and O. M. Yaghi, *Science*, 2017, **355**, eaal1585.
2 C. Ma, X. Li, J. Zhang, Y. Liu and J. J. Urban, *ACS Appl. Mater. Interfaces*, 2020, **12**, 16922.
3 Z. Alsudairy, N. Brown, A. Campbell, A. Ambus, B. Brown, K. Smith-Petty and X. Li, *Mater. Chem. Front.*, 2023, **7**, 3298.
4 G. Zhang, X. Li, Q. Liao, Y. Liu, K. Xi, W. Huang and X. Jia, *Nat. Commun.*, 2018, **9**, 2785.
5 X. Li, H. Wang, H. Chen, Q. Zheng, Q. Zhang, H. Mao, Y. Liu, S. Cai, B. Sun and C. Dun, *Chem*, 2020, **6**, 933.
6 L. Guo, L. Yang, M. Li, L. Kuang, Y. Song and L. Wang, *Coord. Chem. Rev.*, 2021, **440**, 213957.
7 Z. Alsudairy, Q. Zheng, N. Brown, R. Behera, C. Yang, M. Hanif Uddin, A. Saintlima, L. Middlebrooks, J. Li, C. Ingram and X. Li, *Chem. Eng. J.*, 2024, **485**, 149135.
8 H. Xu, S. Tao and D. Jiang, *Nat. Mater.*, 2016, **15**, 722.
9 S. J. Lyle, P. J. Waller and O. M. Yaghi, *Trends Chem.*, 2019, **1**, 172.
10 D. Mullangi, S. Nandi, S. Shalini, S. Sreedhala, C. P. Vinod and R. Vaidhyanathan, *Sci. Rep.*, 2015, **5**, 10876.
11 Y. Li, Y. Han, M. Chen, Y. Feng and B. Zhang, *RSC Adv.*, 2019, **9**, 30937.
12 Y. Kumar, I. Ahmad, A. Rawat, R. K. Pandey, P. Mohanty and R. Pandey, *ACS Appl. Mater. Interfaces*, 2024, **16**, 11605.
13 X. Li, C. Yang, B. Sun, S. Cai, Z. Chen, Y. Lv, J. Zhang and Y. Liu, *J. Mater. Chem. A*, 2020, **8**, 16045.
14 J. Hu, Z. Huang and Y. Liu, *Angew. Chem., Int. Ed.*, 2023, **62**, e202306999.
15 J.-L. Do and T. Friščić, *ACS Cent. Sci.*, 2017, **3**, 13.
16 T. Friščić, C. Mottillo and H. M. Titi, *Angew. Chem.*, 2020, **132**, 1030.
17 A. Krusenbaum, S. Grätz, G. T. Tigineh, L. Borchardt and J. G. Kim, *Chem. Soc. Rev.*, 2022, **51**, 2873.
18 S. Głowniak, B. Szczęśniak, J. Choma and M. Jaroniec, *Mater. Today*, 2021, **46**, 109.
19 B. P. Biswal, S. Chandra, S. Kandambeth, B. Lukose, T. Heine and R. Banerjee, *J. Am. Chem. Soc.*, 2013, **135**, 5328.
20 G. Das, D. B. Shinde, S. Kandambeth, B. P. Biswal and R. Banerjee, *Chem. Commun.*, 2014, **50**, 12615.
21 S. Karak, S. Kandambeth, B. P. Biswal, H. S. Sasmal, S. Kumar, P. Pachfule and R. Banerjee, *J. Am. Chem. Soc.*, 2017, **139**, 1856.
22 S. Hutsch, A. Leonard, S. Graetz, M. V. Höfler, T. Gutmann and L. Borchardt, *Angew. Chem., Int. Ed.*, 2024, e202403649.
23 E. Hamzehpoor, F. Effaty, T. H. Borchers, R. S. Stein, A. Wahrhaftig-Lewis, X. Ottenwaelder, T. Friščić and D. F. Perepichka, *Angew. Chem., Int. Ed.*, 2024, e202404539.
24 N. Brown, Q. Zhang, Z. Alsudairy, C. Dun, Y. Nailwal, A. Campbell, C. Harrod, L. Chen, S. Williams, J. J. Urban, Y. Liu and X. Li, *ACS Sustainable Chem. Eng.*, 2024, **12**, 13535.
25 Y. Nailwal, Q. Zhang, N. Brown, Z. Alsudairy, C. Harrod, M. H. Uddin, F. Akram, J. Li, Y. Liu and X. Li, *Chem. – Eur. J.*, 2025, **31**, e202500339.
26 Y. Jiao, Y. Nan, Z. Wu, X. Wang, J. Zhang, B. Zhang, S. Huang and J. Shi, *Appl. Mater. Today*, 2022, **26**, 101381.
27 Y. Guo, X. Liu, X. Liu, N. Xu and X. Wang, *Dalton Trans.*, 2023, **52**, 12264.
28 X. Zhao, P. Pachfule, S. Li, T. Langenhahn, M. Ye, G. Tian, J. Schmidt and A. Thomas, *Chem. Mater.*, 2019, **31**, 3274.
29 S. A. Patil, R. R. Rodríguez-Berríos, D. Chavez-Flores, D. V. Wagle and A. Bugarin, *ACS ES&T Water*, 2023, **3**, 2009.
30 T. Pan, K. Yang, X. Dong and Y. Han, *J. Mater. Chem. A*, 2023, **11**, 5460.
31 X. Guo, Y. Tian, M. Zhang, Y. Li, R. Wen, X. Li, X. Li, Y. Xue, L. Ma, C. Xia and S. Li, *Chem. Mater.*, 2018, **30**, 2299.
32 M. Zhang, Y. Li, W. Yuan, X. Guo, C. Bai, Y. Zou, H. Long, Y. Qi, S. Li, G. Tao, C. Xia and L. Ma, *Angew. Chem., Int. Ed.*, 2021, **60**, 12396.
33 N. Farooq, A. Taha and A. A. Hashmi, *J. Mater. Chem. A*, 2024, **12**, 10539.
34 N. Brown, Z. Alsudairy, R. Behera, F. Akram, K. Chen, K. Smith-Petty, B. Motley, S. Williams, W. Huang, C. Ingram and X. Li, *Green Chem.*, 2023, **25**, 6287.
35 M. Zhang, J. Chen, S. Zhang, X. Zhou, L. He, M. V. Sheridan, M. Yuan, M. Zhang, L. Chen, X. Dai, F. Ma, J. Wang, J. Hu, G. Wu, X. Kong, R. Zhou, T. E. Albrecht-Schmitt, Z. Chai and S. Wang, *J. Am. Chem. Soc.*, 2020, **142**, 9169.
36 S. T. Emmerling, L. S. Germann, P. A. Julien, I. Moudrakovski, M. Etter, T. Friščić, R. E. Dinnebier and B. V. Lotsch, *Chem*, 2021, **7**, 1639.
37 X. Li, Z. Jia, J. Zhang, Y. Zou, B. Jiang, Y. Zhang, K. Shu, N. Liu, Y. Li and L. Ma, *Chem. Mater.*, 2022, **34**, 11062.
38 K. Wang, X. Qiao, H. Ren, Y. Chen and Z. Zhang, *J. Am. Chem. Soc.*, 2025, **147**, 8063.
39 J. Hu, S. K. Gupta, J. Ozdemir and H. Beyzavi, *ACS Appl. Nano Mater.*, 2020, **3**, 6239.
40 C. Ji, C. Kang, B. C. Patra and D. Zhao, *CCS Chem.*, 2024, **6**, 856.
41 R. K. Jetti, P. K. Thallapally, A. Nangia, C.-K. Lam and T. C. Mak, *Chem. Commun.*, 2002, 952.
42 L. Xu, S.-Y. Ding, J. Liu, J. Sun, W. Wang and Q.-Y. Zheng, *Chem. Commun.*, 2016, **52**, 4706.
43 A. Khojastehnezhad, K. Rhili, M. K. Shehab, H. Gamraoui, Z. Peng, A. Samih ElDouhaibi, R. Touzani, B. Hammouti, H. M. El-Kaderi and M. Siaj, *ACS Appl. Energy Mater.*, 2023, **6**, 12216.
44 J. Yang, S. Ghosh, J. Roeser, A. Acharjya, C. Penschke, Y. Tsutsui, J. Rabeah, T. Wang, S. Y. Djoko Tameu, M.-Y. Ye, J. Grüneberg, S. Li, C. Li, R. Schomäcker, R. Van De Krol, S. Seki, P. Saalfrank and A. Thomas, *Nat. Commun.*, 2022, **13**, 6317.
45 X. Guan, Z. Shen, L. Chen, C. Zhang, C. Sun, Y. Du, B. Hu and C. Gao, *ACS Appl. Nano Mater.*, 2024, **7**, 27318.
46 Z. Wang and Y. Huang, *New J. Chem.*, 2023, **47**, 3668.
47 H. Li, D. Zhang, K. Cheng, Z. Li and P.-Z. Li, *ACS Appl. Nano Mater.*, 2023, **6**, 1295.
48 S. An, X. Zhu, Y. He, L. Yang, H. Wang, S. Jin, J. Hu and H. Liu, *Ind. Eng. Chem. Res.*, 2019, **58**, 10495.

49 A. Gogia, P. Das and S. K. Mandal, *ACS Appl. Mater. Interfaces*, 2020, **12**, 46107.

50 A. Gogia, H. Bhambri and S. K. Mandal, *ACS Appl. Mater. Interfaces*, 2023, **15**, 8241.

51 D. Chen, T. Ma, X. Zhao, X. Jing, R. Zhao and G. Zhu, *ACS Appl. Mater. Interfaces*, 2022, **14**, 47126.

52 Y. Zhao, X. Liu, Y. Li, M. Xia, T. Xia, H. Sun, Z. Sui, X.-M. Hu and Q. Chen, *Microporous Mesoporous Mater.*, 2021, **319**, 111046.

53 B. Mishra, S. Dutta, U. Pal, S. Rana, S. K. Mishra, T. Saha-Dasgupta and P. Pachfule, *Small*, 2025, **21**, 2411199.

54 Y. Yang, X. Xiong, Y. Fan, Z. Lai, Z. Xu and F. Luo, *J. Solid State Chem.*, 2019, **279**, 120979.

55 N. Mokhtari and M. Dinari, *Sep. Purif. Technol.*, 2022, **301**, 121948.

56 S. Ruidas, A. Chowdhury, A. Ghosh, A. Ghosh, S. Mondal, A. D. D. Wonanke, M. Addicoat, A. K. Das, A. Modak and A. Bhaumik, *Langmuir*, 2023, **39**, 4071.

57 H. Bhambri and S. K. Mandal, *ACS Appl. Energy Mater.*, 2023, **6**, 12307.

58 P. Chen, X. He, M. Pang, X. Dong, S. Zhao and W. Zhang, *ACS Appl. Mater. Interfaces*, 2020, **12**, 20429.

59 B. Guo, F. Li, C. Wang, L. Zhang and D. Sun, *J. Mater. Chem. A*, 2019, **7**, 13173.

60 Y. Lin, P. Zeng, D. Wang, T.-T. Li, L.-H. Wu and S.-R. Zheng, *Dalton Trans.*, 2023, **52**, 7709.